

Identification and Localization of Polycystin, the *PKD1* Gene Product

Lin Geng,* Yoav Segal,* Bernard Peissel,* Nanhua Deng,[‡] York Pei,[§] Frank Carone,^{||} Helmut G. Rennke,[¶] Alexandra M. Glücksmann-Kuis,[‡] Michael C. Schneider,* Maria Ericsson,** Stephen T. Reeders,* and Jing Zhou*

*Renal Division, Brigham and Women's Hospital, Harvard Medical School, Boston, Massachusetts 02115; [‡]Millennium Inc., Boston, Massachusetts 02115; [§]Department of Medicine, University of Toronto, Toronto, Ontario M5G2C4, Canada; ^{||}Department of Pathology, Northwestern University Medical School, Chicago, Illinois 60611; [¶]Department of Pathology, Brigham and Women's Hospital, Harvard Medical School, Boston, Massachusetts 02115; and **Department of Cell Biology, Harvard Medical School, Boston, Massachusetts 02115

Abstract

Polycystin, the product of autosomal dominant polycystic kidney disease (ADPKD) 1 gene (*PKD1*) is the cardinal member of a novel class of proteins. As a first step towards elucidating the function of polycystin and the pathogenesis of ADPKD, three types of information were collected in the current study: the subcellular localization of polycystin, the spatial and temporal distribution of the protein within normal tissues and the effects of ADPKD mutations on the pattern of expression in affected tissues. Antisera directed against a synthetic peptide and two recombinant proteins of different domains of polycystin revealed the presence of an ~400-kD protein (polycystin) in the membrane fractions of normal fetal, adult, and ADPKD kidneys. Immunohistological studies localized polycystin to renal tubular epithelia, hepatic bile ductules, and pancreatic ducts, all sites of cystic changes in ADPKD, as well as in tissues such as skin that are not known to be affected in ADPKD. By electron microscopy, polycystin was predominantly associated with plasma membranes. Polycystin was significantly less abundant in adult than in fetal epithelia. In contrast, polycystin was overexpressed in most, but not all, cysts in ADPKD kidneys. (*J. Clin. Invest.* 1996. 98:2674–2682.) **Key words:** antibodies • subcellular localization • kidney development • cystic disease • electron microscope

Introduction

Autosomal dominant polycystic kidney disease (ADPKD)¹ is a common monogenic disease of man, affecting approximately 1 in 1,000 individuals. The most common manifestation is cystic

replacement of renal tissue leading to progressive renal failure, and requiring renal replacement therapy in half of the cases by age 50 (1). ADPKD is a systemic disease affecting many tissues besides the kidney; for example, hepatic and pancreatic cysts are common although rarely symptomatic. An association with intracranial aneurysms and heart valve defects has also been reported (2).

ADPKD is caused by mutations in at least three genes. The *PKD1* and *PKD2* genes have been mapped to chromosomes 16 (3) and 4, respectively (4, 5). The third locus has not been identified (6). Mutations in *PKD1* account for ~90% of ADPKD cases. *PKD1* produces a 14-kb transcript encoding a 4304-residue protein, designated polycystin (7, 8). Polycystin contains an NH₂-terminal signal peptide which is followed by two leucine-rich repeats (LRR), a C-lectin domain, and an LDL-A domain. These domains are followed by a tandem array of 13 copies of a novel 80-residue "PKD" domain. COOH-terminal to the PKD domains is a hydrophobic region containing 9–11 putative membrane-spanning segments, and an intracellular domain of ~200 residues. This unique combination of domains defines polycystin as the cardinal member of a newly identified class of proteins.

As an initial approach towards elucidating the pathogenesis of ADPKD, we have carried out immunobiochemical and immunohistochemical analyses of polycystin expression. We raised antibodies against a synthetic peptide and two recombinant proteins of polycystin to study its subcellular localization and tissue distribution in normal and ADPKD tissues. We provide the first biochemical and ultrastructural evidence that polycystin is a membrane-associated ~400 kD molecule. In the kidney, polycystin is expressed in the tubules where it is found on both the apical and basolateral domains of the plasma membranes of polarized epithelia. In kidneys from 15 ADPKD patients, we found overexpression of polycystin in the large majority of cysts.

Methods

Generation of fusion proteins. Fusion protein MR3R, containing a portion of the putative first extracellular loop of human polycystin, was generated by subcloning a fragment of *PKD1* cDNA (nucleotides 8956–9261, amino acids 2985–3086) (7, 8) into the pMAL-C2 expression vector immediately following the Xa cleavage site according to manufacturer's instructions (New England Biolabs, Beverly, MA). Fusion protein PKCR, containing a portion of the intracellular domain at the extreme COOH terminus of murine polycystin (homologous *PKD1* cDNA sequence nucleotides 12478–13137) was prepared in a similar manner.

Address correspondence to Jing Zhou, M.D., Ph.D., Renal Division, Department of Medicine, Brigham and Women's Hospital, Harvard Medical School, Boston, MA 02115. Phone: 617-278-0331; FAX: 617-732-6392; E-mail: zhou@mberr.harvard.edu

Received for publication 8 April 1996 and accepted in revised form 29 August 1996.

1. Abbreviation used in this paper: ADPKD, autosomal dominant polycystic kidney disease.

J. Clin. Invest.

© The American Society for Clinical Investigation, Inc.

0021-9738/96/12/2674/09 \$2.00

Volume 98, Number 12, December 1996, 2674–2682

Antibodies. Polyclonal antibodies against chemically synthesized peptide MR3 (EPYLAVYLHSEPRNEHN, amino acids 2938–2956) (7, 8) and fusion proteins were raised in New Zealand white rabbits. MR3 peptide was chosen because (a) it has high predicted antigenicity, (b) it shows no homology to known proteins (7, 8), and (c) it is extracellular. Two rabbits were immunized with 0.1 mg of each antigen. Mouse monoclonal antibodies against human $\alpha 1(\text{IV})$ type IV collagen and anti- α -actin, a vascular smooth muscle antigen, were purchased from Sigma Chemical Co. (St. Louis, MO). Mouse monoclonal anti-human antibody Uro5 was purchased from Signet (Dedham, MA). Uro5 antigen is a 48-kD glycoprotein found in a portion of Henle's loop, distal tubules, and collecting ducts of the kidney but not the proximal tubules.

Affinity purification. All polyclonal antibodies were purified using membrane bound fusion proteins. Briefly, fusion proteins were electrophoresed on a 10% SDS-PAGE and electrotransferred onto PVDF immobilon-p membranes (Millipore Corp., Bedford, MA). Antisera were incubated with the membrane overnight and washed in buffer (500 mM NaCl, 10 mM Tris-HCl, pH 7.5, 0.2% Triton X-100) three times at room temperature. The bound antibodies were eluted in 0.1M glycine-HCl, pH 3.2. Antisera against fusion proteins were first affinity-purified with a maltose binding protein coupled column. Affinity-purified antibodies were designated pMR3-Ab, pMR3R-Ab and pPKCR-AB, respectively. The reactivity of the affinity-purified antibodies was shown by blotting with the fusion protein.

Tissues and patient materials. Fetal tissues of 14–22 week gestation were obtained at necropsy. Adult tissues were removed during tumor resections. ADPKD kidneys were obtained at nephrectomy. Two families (BC and RS) have been shown to be linked to chromosome 16 by linkage analysis. For immunofluorescence and immunoperoxidase studies, the tissue blocks were immediately frozen in liquid nitrogen, embedded in OCT compound (Miles, Elkhart, IN), and stored at -80°C .

Isolation of human kidney membranes. Fetal and adult kidneys were homogenized in HB buffer (10 mM phosphate buffer, 20 mM KCl, 5% sucrose, 0.5 mM MgCl_2 , 1 mM EDTA, 1 mM EGTA, 1 mM DTT, 1 mM PMSF, 5 $\mu\text{g/ml}$ pepstatin A, 5 $\mu\text{g/ml}$ antipain, 2.5 $\mu\text{g/ml}$ leupeptin) with either a pestle and mortar or a tissue homogenizer. Tissue homogenates were centrifuged successively at 1,000g for 15 min, 8,000 g for 20 min and 100,000 g for 2 h. Supernatant (S100) and pellet fractions (P100 and P8) were collected. Pellets were resuspended in HB buffer, snap frozen in liquid nitrogen, and stored at -80°C . All steps were performed at 4°C . Protein concentrations were measured by the Bradford method.

Western blotting. Protein samples (5–10 μg of fusion proteins or 100–200 μg of tissue fractions) were solubilized in sample buffer (2% SDS, 30 mM Tris-HCl, pH 6.8, 5% 2-Mercaptoethanol, 12% (vol/vol) glycerol) and electrophoretically fractionated on 5–15% SDS-PAGE gradients or on 5% or 10% SDS-PAGE gels with or without boiling. Proteins were electrotransferred to PVDF immobilon-p membranes (Millipore Corp.) and blotted with specific antibodies (MR3-Ab and MR3R-Ab at 1:1000 dilution, purified antisera at 1:3 or 1:10) in blotting buffer (5% nonfat dry milk in 0.15 M NaCl, 1% Triton X-100, and 20 mM Tris-HCl pH 7.4). After several washes, the membranes were incubated with peroxidase-conjugated secondary antibody, and detected by enhanced chemiluminescence (ECL, Amersham, UK).

Immunocytochemistry. Tissues embedded in OCT compound were sectioned at 5 μm in a cryostat at -20°C . Sections were air dried for 30 min, and then fixed in acetone for 5 min. After brief air drying, the sections were rinsed three times in PBS and incubated with 20 μl of primary antibody for one hour. MR3-Ab and MR3R-Ab antisera were used at a dilution of 1:100. Monoclonal antibodies were used at 1:4–1:20. Control sections were incubated with pre-immune serum (MR3) or with normal mouse IgG at the same concentration. For antigen blocking experiments, the same dilutions of antibodies were pre-incubated with a specific antigen (either in solution or on immunoblot) for 1 h at room temperature. After washing, the sections were incubated for 45 min with 20 μl of the appropriate secondary antibody,

either FITC-conjugated goat anti-rabbit IgG (Sigma Chemical Co.) or Texas red-conjugated goat anti-mouse IgG (sheep to rabbit IgG [Cappel, Durham, NC], or goat anti-mouse IgG and IgM [Jackson ImmunoResearch, West Grove, PA]) for 30 min at room temperature. Dual label experiments were carried out by mixing the two primary or the secondary antibodies, respectively. Sections were mounted in glycerol and PBS and observed with epifluorescent illumination.

For immunoperoxidase staining, the primary polyclonal antibodies were diluted to 1:500 while monoclonal antibodies were diluted to 1:20. Immunoperoxidase staining was carried out using the Vectastain Elite ABC kit (Vector, Burlingame, CA) containing avidin DH and biotinylated horseradish peroxidase. Biotinylated goat anti-mouse IgG and goat anti-rabbit IgG (Vector) were used as second antibodies. Diaminobenzidine tetrahydrochloride was used as a chromogen and methyl green was used for counterstaining (Sigma Chemical Co.). Photographs were taken with a Nikon 200 and Kodak T-MAX 400 ISO films.

Immunogold-electron microscopy. For cryosections the tissue was fixed in 2% paraformaldehyde (in 200 mM Hepes, pH 7.4) overnight, cut into small pieces and infiltrated with PVP-sucrose (9) for 1 h at room temperature prior to plunge-freezing in liquid nitrogen. Ultrathin cryosections were cut at -120°C on a Reichert Ultracut S microtome. Sections were collected from the knife with a loop dipped in a 3:2 mixture of 2.3 M sucrose and 2% methyl cellulose, placed on a formvar-carbon coated grid and transferred to PBS. Immunogold labeling was carried out as described (10).

Quantitation of immunogold labeling. 20 micrographs of randomly sampled regions of renal tubules were taken at a primary magnification of 12,000. The specific density of the label per linear trace of membrane was determined by counting gold particles falling within two membrane widths of the membrane and intersection of the membrane with a series of test lines, as described by Griffiths (11). A *t* test analysis was used to determine the significance of the difference of the labeling density on the apical and basolateral membranes.

Results

Generation and characterization of anti-polycystin antisera. Three different immunogens, a synthetic peptide and two fusion proteins, were used to obtain rabbit polyclonal antisera to polycystin. All three antisera gave very similar results in Western analysis and immunolocalization. Antiserum MR3-Ab was raised against MR3, an 18-residue synthetic peptide taken from the deduced amino acid sequence of polycystin (see Methods). Antiserum MR3R-Ab was raised against MR3R, a maltose-binding protein (MBP)-tagged fusion protein containing 100 residues of the first extracellular loop of the putative transmembrane region of polycystin (8) which includes MR3. A third antibody, PKCR-Ab, raised against a fusion protein containing the extreme COOH terminus of murine polycystin (PKCR), was used to confirm the findings obtained with MR3-Ab and MR3R-Ab.

The specificities of the antibodies were demonstrated in a series of experiments. MR3-Ab was found to bind strongly to the MR3 peptide by ELISA (data not shown); by Western analysis, MR3-Ab bound strongly to the cleaved polycystin peptide, but not to MBP nor to a fusion protein containing the COOH terminus of murine polycystin (Fig. 1, A and B). The binding was inhibited by absorption of the antisera with specific antigen, MR3. Pre-immune sera from the same rabbit did not show reactivity (Fig. 1 B). Binding of MR3R-Ab and PKCR-Ab to the immunizing peptides was blocked by pre-incubation with their specific antigens (data not shown).

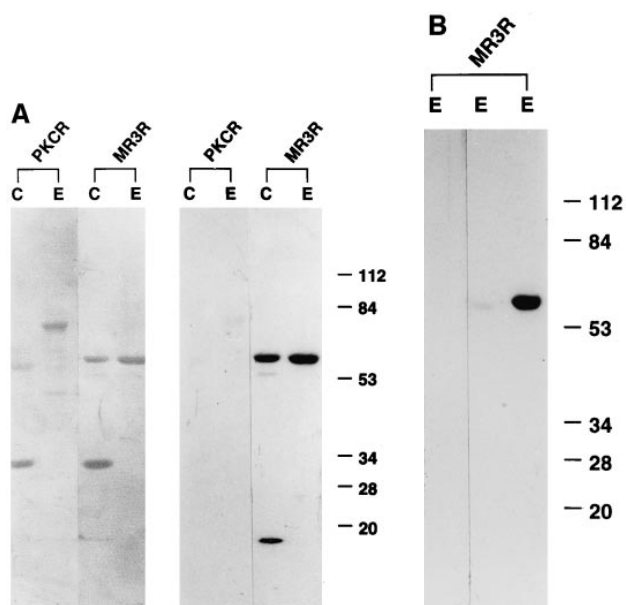


Figure 1. Specificity of polyclonal antibody MR3-Ab. (A) Western blot of 10% SDS-PAGE gel of recombinant fusion protein PKCR and MR3R. MR3-Ab (*right*) reacted strongly with the cleaved (C) (~ 11 kD) and uncleaved (E) fusion protein MR3R (~ 53 kD) but not with the 34-kD maltose binding protein seen by Coomassie blue staining (*left*) nor with PKCR, a recombinant protein of the extreme COOH terminus of murine polycystin. (B) Immunoabsorption of MR3-Ab with MR3 peptide abolished the binding of MR3-Ab to MR3R (*middle lane*). Pre-immune sera did not show any binding (*left lane*). Control immune serum exhibited strong binding to the fusion protein (*right lane*).

Identification and subcellular localization of polycystin.

We focused our biochemical analysis on renal tissues, the site of the major pathology in ADPKD. Total tissue homogenates were prepared from three normal 18–22-wk normal fetal kidneys, one normal adult kidney and five ADPKD kidneys from unrelated individuals. A large molecular weight protein was detected in the P8 and P100 membrane fractions by both MR3-Ab and MR3R-Ab. Further analysis of membrane fractions on 5% SDS-PAGE gels under reducing and nonreducing conditions revealed that the protein is ~ 400 kD, similar to the predicted size of polycystin encoded by the longest open reading frame of *PKD1* (~ 460 kD). This protein was detected by both purified and unpurified MR3-Ab and MR3R-Ab (Fig. 2, A and B, and data not shown), which are targeted at an extracellular loop of the putative transmembrane domain, as well as by PKCR-Ab, which is targeted at the putative intracellular domain (Fig. 2 C). All three antibodies also detected a band of ~ 200 kD in some ADPKD and fetal kidney homogenates; however, the intensity of this band varied markedly between homogenates prepared from the same tissue sample, suggesting that it represents a proteolytic cleavage product rather than a second isoform or homologue of polycystin. Detection of both the 400- and 200-kD bands could be blocked by pre-incubation of the antibodies with appropriate antigens but not with unrelated antigens (Fig. 2 D, and data not shown). Pre-immune sera did not display reactivity. The level of polycystin was similar in the fetal and ADPKD kidney homogenates but significantly lower in adult kidneys (Fig. 2).

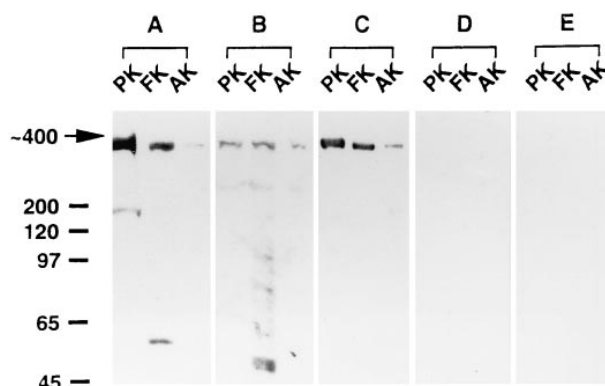


Figure 2. Identification of the protein product of the *PKD1* gene in normal and ADPKD kidneys. Aliquots (~ 100 µg) of P100 fraction from 18–22-wk normal human fetal kidneys (FK), normal adult kidneys (AK), and an ADPKD kidneys (PK) were subjected to 5% SDS-PAGE and immunoblotted with (A) pMR3-Ab; (B) pMR3R-Ab; (C) pPKCR-Ab. A low abundance protein of ~ 400 kD was detected by all three antibodies. The small molecular bands (e.g., 200 kD) are probably degradation products. (D) Binding of pPKCR-Ab to the same tissue samples was blocked by pre-incubation with its antigen. (E) Pre-immune sera did not show any reactivity. Molecular weight standards (BRL, Bethesda, MD) are indicated on the left.

Localization of polycystin in normal tissues and ADPKD kidneys. MR3-Ab gave intense staining in tissue sections whereas the other two antibodies gave weaker but similar results; MR3-Ab was, therefore, used in immunolocalization studies. Reactivity of MR3-Ab with tissue sections was blocked by pre-incubation with MR3R and the 400-kD protein fixed on membranes (see Methods and data not shown). In summary, polycystin was found in restricted, non-contiguous segments of the renal tubule in fetal kidney: a portion of Bowman’s capsule contiguous with the proximal tubule, the proximal tubule itself and the collecting duct. Polycystin was found in the ureteric ducts but was absent from the uninduced mesenchyme, nephrogenic condensates, and renal vesicles. It first appears in the S-shaped bodies but is not expressed in the glomerulus during development. In adult kidneys, polycystin was also shown to be limited to tubular structures, but was found at much lower levels. By contrast, in kidneys from patients with ADPKD the vast majority of cysts stained heavily for polycystin. Adjacent nondilated tubules stained weakly. Polycystin was found in a range of other organs including the epithelial cell surfaces of small biliary ductules and pancreatic ducts. Both these structures are common sites of cystic dilatation in ADPKD. In skin, polycystin was confined to the basal keratinocytes. The results are described in detail below.

Fetal kidney. We examined tissues from 11-, 14-, 15-, 18-, 19-, 21-, and 22-wk human fetuses. High levels of polycystin expression were found in the epithelia of ureter-derived structures: ureteric buds and collecting ducts (Fig. 3, A–K). Staining was weaker in the tips of the ureteric buds where induction of mesenchymal-epithelial transformation occurs (Fig. 3, A, B, and D). Polycystin staining was absent from the uninduced metanephric mesenchyme, nephrogenic condensates and renal vesicles. Expression in mesenchyme-derived structures first appears in the S-shaped bodies (Fig. 3, A and E). Polycystin was not observed in the developing or mature glomeruli but

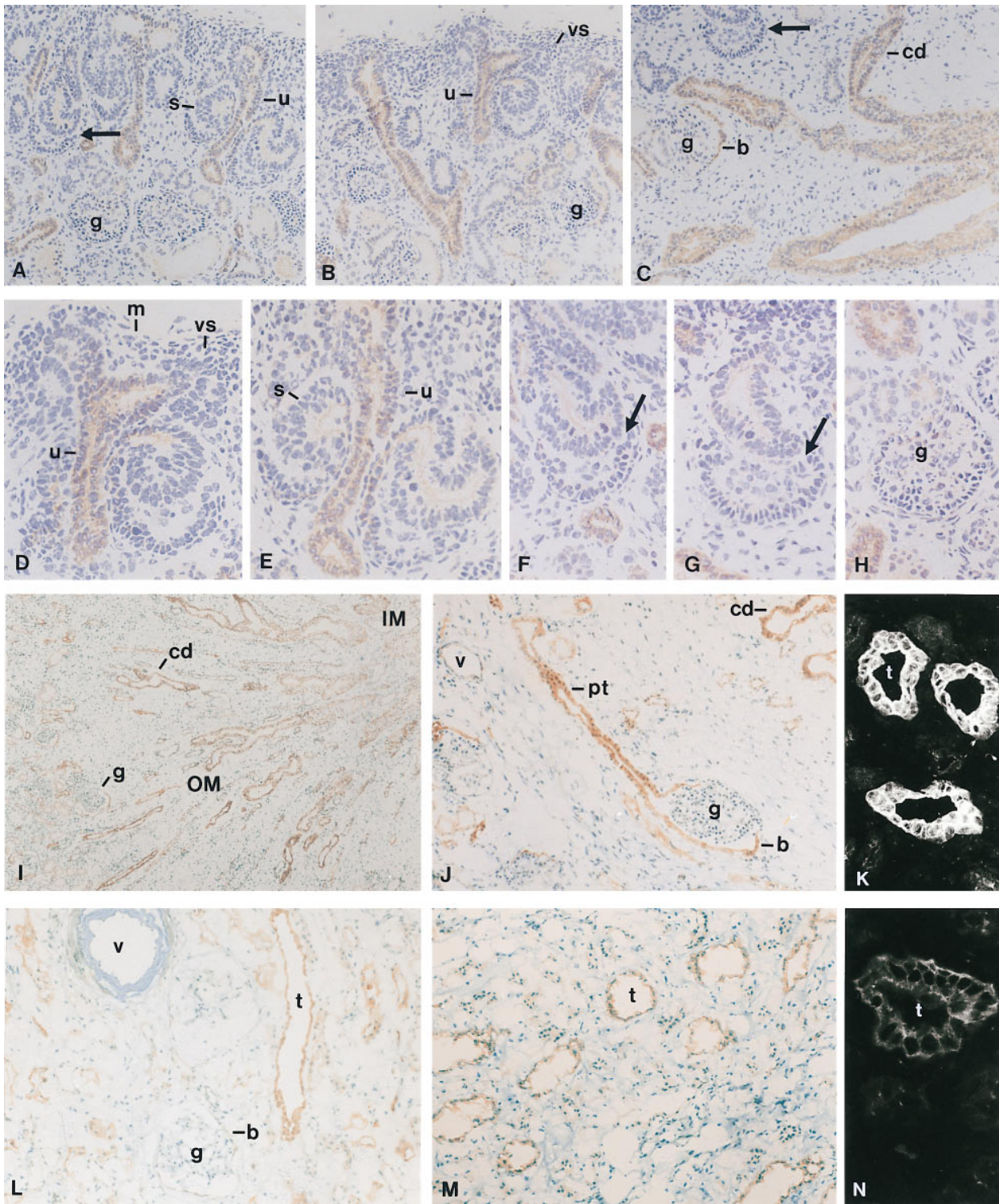


Figure 3. Tissue localization of polycystin in fetal (A–K), and adult (L–N) kidneys using rabbit anti-human polycystin antibody MR3-Ab by immunoperoxidase (A–J, L, and M) and immunofluorescence (K and N). In 14-wk fetal kidney (A–H), polycystin is seen in the branching ureteric ducts (*u*), collecting ducts (*cd*), and Bowman's capsules (*b*). Trace labeling is seen in S-shaped bodies (*s*). Polycystin is absent from the uninduced mesenchyme (*m*), nephrogenic condensates, renal vesicles (*vs*) and various stages of developing glomeruli (capillary loop stage, *arrow*; mature glomerulus, *g*). In 18-wk fetal kidney (I–K), polycystin is highly expressed in the collecting system and proximal tubules (*pt*). Subtle decrease of polycystin staining in large collecting ducts in inner medulla is seen (I). In adult kidney (L–N), a subset of tubules (*t*) present in both the cortex (L and N) and medulla (M) are stained. Weak labeling is seen in Bowman's capsule (*b*) but not in the glomerulus. Vessels (*v*) do not express polycystin in either fetal or adult kidneys (J and L). Polycystin expressing tubules in fetal (K) or adult (N) kidneys are shown by immunofluorescence staining. *IM*, inner medulla, *OM*, outer medulla. A–C, J, L, and M, $\times 75$; D–H, $\times 150$; I, $\times 30$; K and N, $\times 300$.

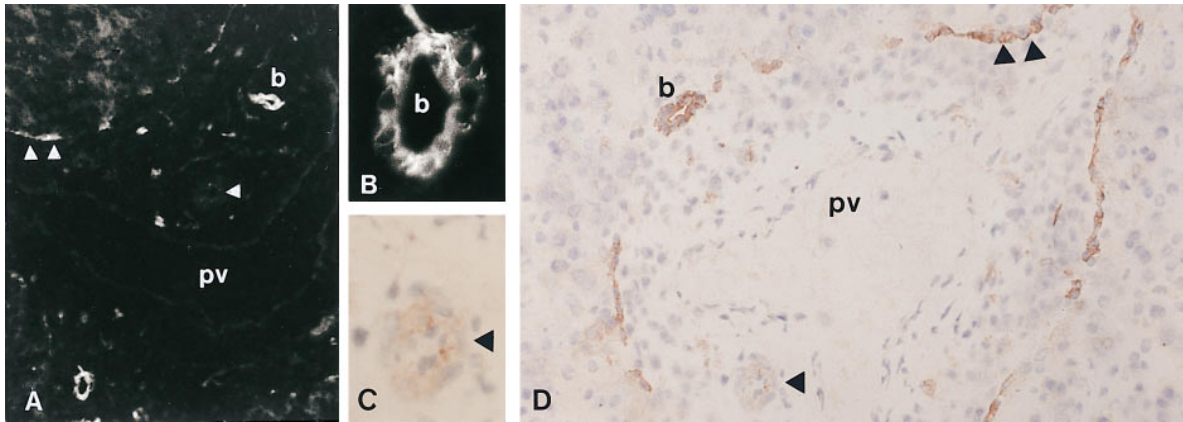


Figure 4. Tissue localization of polycystin in 18-wk fetal liver (A–D) using rabbit anti-human polycystin antibody MR3-Ab. Only bile ductules (b) and ductal plates (double arrowheads) are stained (A, B, and D). Portal veins (pv), hepatic arteries (arrowhead), hepatocytes and lymphatics are not stained (A, C, and D). A, $\times 75$; B and C, $\times 300$; D, $\times 150$.

staining was present in portions of Bowman’s capsules contiguous with the proximal tubules and in the proximal tubules themselves (Fig. 3 J).

Polycystin seems to be expressed on the cell surfaces of epithelia. Staining appeared to be more intense on the apical surfaces; the distribution between apical and basolateral membranes was studied quantitatively by electron microscopy (vide infra). Cytoplasmic staining was also seen (Fig. 3, A–K) but polycystin is clearly absent from the nucleus (Fig. 3 K). Electron microscopy suggests that the majority of cytoplasmic polycystin is associated with membrane structures (vide infra).

A similar pattern of expression was seen in all stages of development we examined; however, from 18 weeks of gestation onwards, staining of the large collecting ducts starts to de-

crease slightly (Fig. 3 I). The blood vessels were not stained (Fig. 3 J); absence of staining was confirmed by dual labeling of polycystin and α -actin (data not shown).

Adult kidney. The expression of polycystin was studied in five normal adult kidneys. Polycystin was clearly present in the adult kidney, but the level of expression was generally lower than that in fetal kidneys (Fig. 3, L–N). Polycystin was found in some segments of the tubule both in kidney cortex (Fig. 3 L) and medulla (Fig. 3 M). Counterstaining with marker antibody Uro5 revealed that polycystin was not detected in proximal tubules by immunofluorescence (data not shown). Dual labeling of polycystin and Uro8, a Henle’s loop marker revealed colocalization of both antigens though the level of polycystin expression was very low (data not shown). Polycystin was also

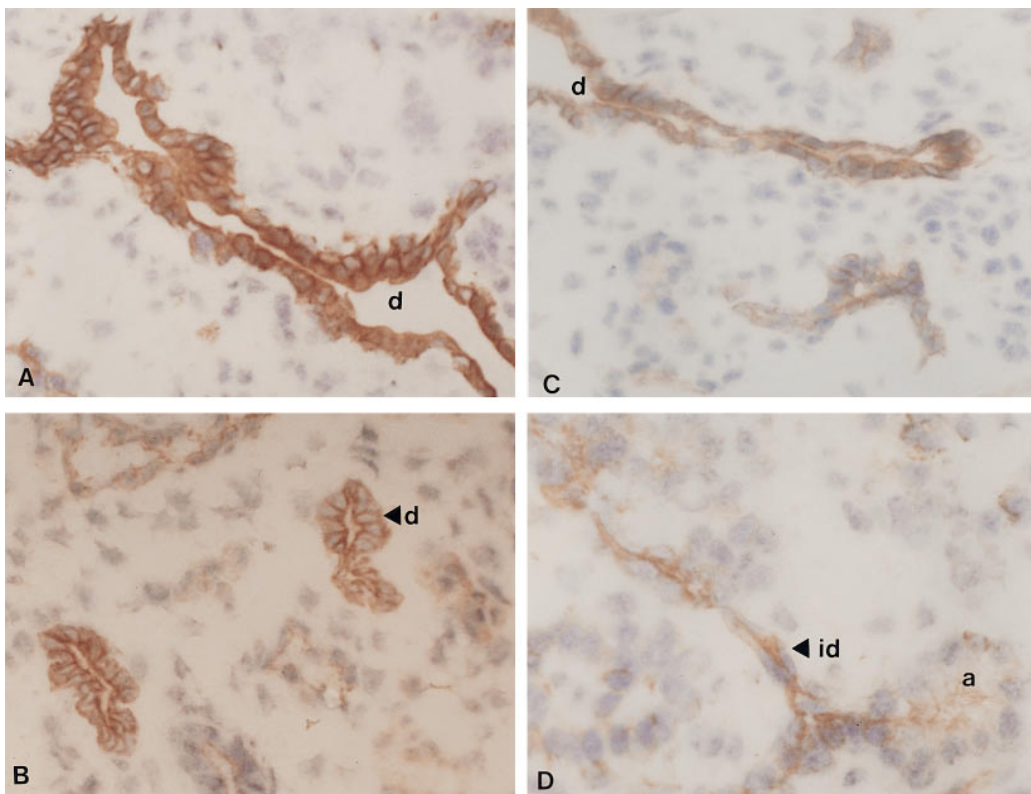


Figure 5. Tissue localization of polycystin in 18-wk fetal pancreas (A–D) using rabbit anti-human polycystin antibody MR3-Ab. Various pancreatic ducts (d) are stained (A–D). Large ducts are more strongly labeled than smaller ducts (A and C). Intercalated ducts (id) are weakly labeled (D). Acinar cells (a) are not labeled. A–C $\times 300$; D $\times 400$.

seen weakly in the Bowman's capsule. Polycystin was absent from the glomeruli and blood vessels (Fig. 3 L).

Fetal liver and pancreas. In 18-wk fetal liver polycystin was found in the epithelial cells of bile ductules and the segmental double-layered ductal plates which form the future bile duct network (Fig. 4, A–D). Polycystin is absent from the mesenchyme surrounding the portal vein and portal vein itself. No detectable polycystin expression was observed in hepatocytes or in hepatic arterioles (Fig. 4, A, C, and D).

In 18-wk fetal pancreas, polycystin was only seen in the epithelial cells of the pancreatic ducts (Fig. 5, A–D). Expression was greater in large than in small ducts. Acinar cells and blood vessels do not express polycystin. Within epithelia, polycystin is predominantly present on the cell surface.

Fetal and adult skin. Although skin is not obviously abnormal in ADPKD, skin is a readily accessible tissue as a source for protein analysis in patients. We therefore examined both fetal and adult skin for polycystin expression. Polycystin was

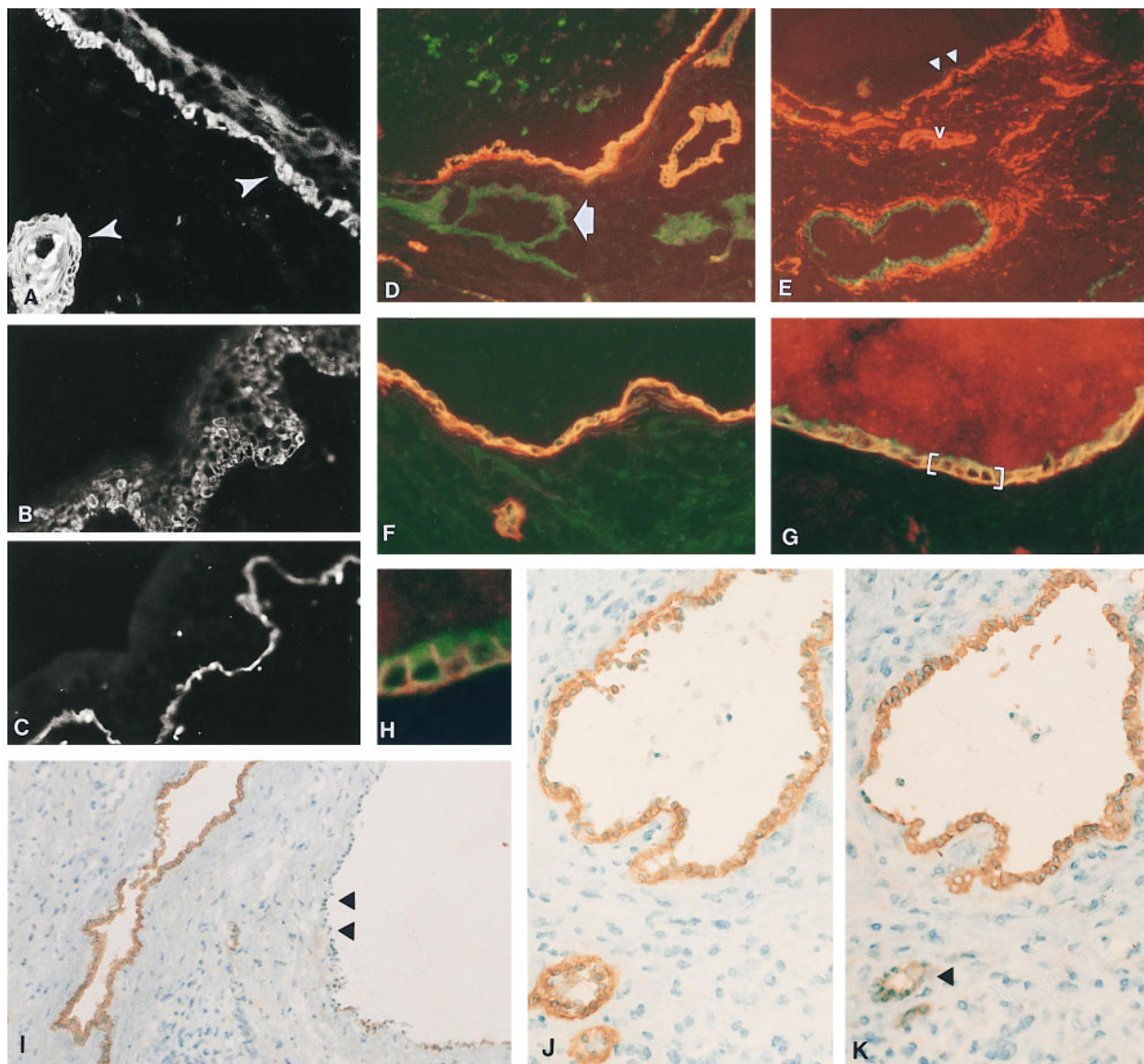


Figure 6. Tissue localization of polycystin in human fetal and adult skin (A–C), and in kidneys from ADPKD patients (D–K) using rabbit anti-human polycystin antibody MR3-Ab. MR3-Ab reacted strongly with the basal keratinocytes (right arrowhead) and hair follicles (left arrowhead) of 18-wk fetal skin (A). Dual labeling of MR3-Ab and mouse anti-human $\alpha 1(IV)$ collagen revealed the presence of polycystin in basal keratinocytes (B) and $\alpha 1(IV)$ collagen in the epidermal basement membranes (C) in adult skin. Various degree of polycystin expression in cysts from ADPKD patients SB (D–F), and BC (G–K) is shown by dual immunofluorescence of polycystin (green) and Uro5 (red, D, F–H); or polycystin (green) and α -smooth muscle actin (red, E), and by immunoperoxidase. Yellow color occurs where the two fluorescent labels exactly codistribute. Polycystin overexpression is seen in most cysts (D–H, green or yellow) but not in $\sim 10\%$ of the cysts (E and I, double arrowheads). Some cysts express polycystin but not Uro5 antigen indicating a proximal tubule origin (D, arrow). Both green and yellow colors are seen in the cyst-lining epithelial cells (H, higher power view of the cells shown in parenthesis in G) indicating that polycystin was present in the same location as Uro5, a cell surface antigen, and in the cytoplasm (D, F–H). Consecutive kidney sections from patient BC stained with Uro5 (J), and polycystin (K) reveals the overexpression of polycystin in a cyst but not in two adjacent nondilated tubules (single arrowhead). Dual labeling of polycystin (green) and α -smooth muscle actin (red) reveals that vessels (v) do not express polycystin (E). A–C, J and K, $\times 150$; D–F, $\times 100$; G, $\times 200$; H, $\times 400$; I, $\times 75$.

found only in the basal keratinocytes of the skin and hair follicles of 18-week fetal skin (Fig. 6 A). Polycystin was not detected in the sweat glands or in the blood vessels. Adult skin has a similar distribution but significantly lower expression than fetal skin (Fig. 6 B).

ADPKD kidneys. In 15 ADPKD kidneys from 15 unrelated individuals (Fig. 6, D–K), polycystin was found to be strongly expressed in epithelia of most, but not all cysts (Fig. 6, D–I, and K). Polycystin was found on the cell surfaces and in the cytoplasm of cystic epithelial cells (Fig. 6, F–H) but not in

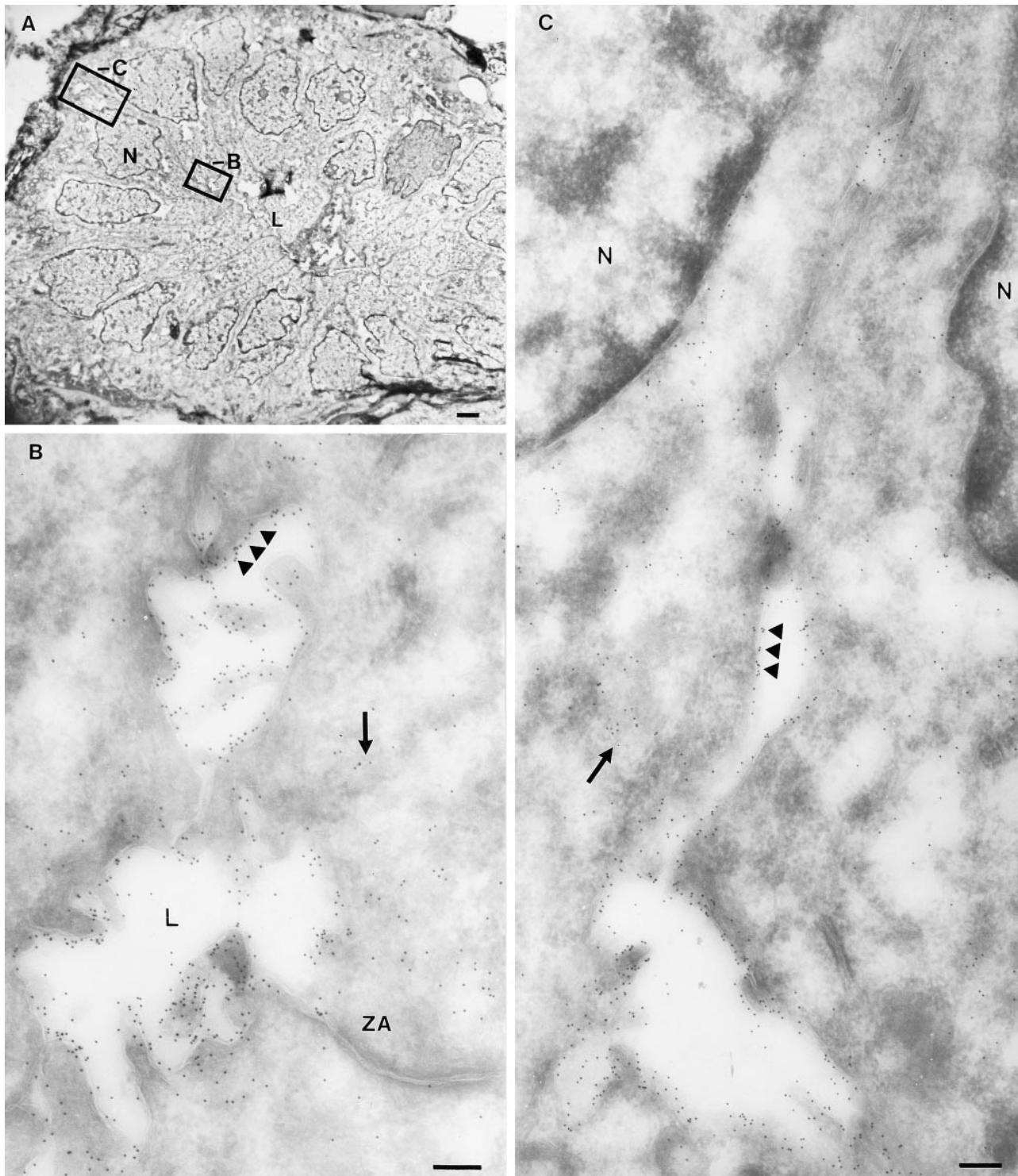


Figure 7. Immunoelectron microscopic localization of polycystin in human fetal kidney of 18-wk using rabbit anti-human polycystin antibody MR3-Ab. MR3-Ab was indirectly labeled with 10nm gold. A cross-section of a tubule is shown in low power (A). Boxes B and C indicate the regions shown at high magnification (B and C). The gold particles are distributed along the apical (B), and basolateral (C) plasma membranes of the tubular epithelial cells (triple arrowheads). L indicates the lumen. ZA, zonula adherence. N, nucleus. Gold particles that are found in the cytoplasm are mostly associated with membranous structures (B, C, arrows). Bar in A, 2 μ m; B and C, 200 nm.

Table I. Density of Polycystin Labeling on Epithelial Plasma Membranes of 18-wk Human Fetal Kidney: Gold/ μm Membrane Length

	MR3	Preimmune
Apical	3.5 \pm 0.4	0.3 \pm 0.03
Basolateral	1.7 \pm 0.3	0.1 \pm 0.02

the vasculature (Fig. 6 E). A small number of cysts with clearly preserved epithelia do not overexpress polycystin (Fig. 6, E and I). To further investigate the variability of polycystin expression in ADPKD kidneys, we carried out a detailed examination of polycystin by immunoperoxidase in four cystic kidneys. Five out of \sim 50 cysts (10%) in a single section were found not to overexpress polycystin (Fig. 6, E and I). The level of polycystin staining in cysts (Fig. 6, D and F–K) did not correlate with the expression of either Uro2 (data not shown) or Uro5, markers of proximal and collecting tubules respectively.

Polycystin is also strongly expressed in some nondilated tubules (Fig. 6 D); further studies will be required to determine whether these are fortuitous sections of cysts or whether they represent increased expression in noncystic nephrons.

Polycystin is intimately associated with epithelial plasma membranes. Immunogold labeling of ultra-thin frozen sections of 18-wk fetal kidneys with either purified or unpurified MR3-Ab showed that polycystin is predominantly present at the plasma membranes of the epithelium of renal tubules (Fig. 7). Particle counts of the apical membranes were significantly greater than the basolateral surfaces ($P < 0.001$) (Table I). Some gold particles were also found in the cytoplasm and appear to be associated with membranous structures. These may represent newly synthesized or recycling protein. As a control, particle counts for preimmune serum were measured in the same fashion (Table I).

Discussion

The primary structure of polycystin, the product of the *PKD1* gene, has recently been deduced. Although polycystin contains several recognizable protein domains, the overall structure of the molecule is unlike any known protein, precluding a provisional assignment of its function. As a first step towards elucidating the function of polycystin and the pathogenesis of ADPKD, three types of information were collected: the subcellular localization of polycystin, the spatial and temporal distribution of the protein within normal tissues and the effects of ADPKD mutations on the pattern of expression in affected tissues.

To verify the specificity of the immunohistochemical studies, antisera were initially raised against two polycystin peptides, MR3 and MR3R. Both antisera recognized an \sim 400-kD protein in the P100 membrane fraction of tissue homogenates and gave virtually identical staining patterns. Furthermore, immunogold labeling localized polycystin to plasma membrane. Antisera raised to a different domain of murine polycystin detected the same band on Western blots providing additional evidence of the specificities of MR3-Ab and MR3R-Ab. Taken together with sequence analysis which suggests the presence of nine to eleven transmembrane domains in polycys-

tin, our data show that, at least one form of polycystin is an integral membrane protein largely found in plasma membranes.

Morphogenesis of the kidney is regulated by reciprocal tissue interactions between the epithelial ureteric bud and the metanephric mesenchyme. Polycystin is expressed in the ureteric bud but is least abundant at the tip of the bud in 14–18-wk fetal kidney suggesting that polycystin is not primarily an inductive signal for mesenchymal-epithelial conversion. Polycystin appears late in kidney development: it is absent from uninduced metanephric blastema, and renal vesicles and starts to appear in S-shaped bodies and primitive tubules at the capillary loop stage; it reaches its peak expression in maturing proximal tubules and collecting ducts. Its expression declines thereafter but is maintained at a low level in mature tubules through adulthood. Based on these findings, we believe that polycystin contributes to the rapid phase of renal tubular growth and plays an important role in the maintenance of epithelia differentiation and tubular architecture. Future independent functional experiments will be required to prove this.

We and others have speculated about the role of polycystin in cyst formation (7, 8). The localization of polycystin makes several popular models of the pathogenesis of ADPKD less likely. For example, the presence of polycystin in epithelial plasma membranes indicates that the ECM abnormalities noted in ADPKD are not likely to be primary defects (12). It has also been suggested that the PKD1 gene product is directly involved in the sorting of membrane proteins (12). This theory drew support from the observation that, in patients with ADPKD, a variety of membrane proteins, including Na⁺, K⁺-ATPase, fodrin, and the EGF receptor are abnormally localized within cyst-lining cells (13–15). The presence of polycystin primarily in cell surface plasma membranes makes it unlikely that polycystin is a sorting protein. In the context of the data presented here, polycystin is more likely to affect cell polarity indirectly, perhaps by mediating interactions between extracellular ligands and intracellular pathways that are important in maintaining epithelial differentiation.

This study shows that polycystin is overexpressed in cysts compared with both non-dilated tubules from the same ADPKD kidney and tubules from normal adult kidneys. This finding was confirmed in kidneys from 15 unrelated individuals from different populations. The size of most of the families does not allow us to carry out linkage analysis in all families and we cannot, therefore, exclude the possibility that one or more of these kidneys contains a *PKD2* or *PKD3* mutation. The polycystin distribution is very similar in all the ADPKD kidneys we tested including 2 documented *PKD1* kidneys. This indicates that it is a common pattern in *PKD1* kidneys. Because of the size of the *PKD1* gene we have not, as yet, determined the nature of the mutations in these patients. Nevertheless, to date, no two unrelated ADPKD patients have been reported to carry the same *PKD1* mutation so that these 15 kidneys are likely to represent a range of different mutations (16–19). Therefore, overexpression of polycystin in cysts appears to be a general property of ADPKD rather than a specific feature of a particular mutation.

One of the intriguing findings in ADPKD is that, although every renal cell contains a mutation, < 10% of tubules contain cysts and, within tubules, cystic dilatation is focal (20, 21). Clearly, some event, the nature of which remains unknown, is responsible for the focal cystic transformation. Is the increase in polycystin levels the trigger for cyst formation or is it a sec-

ondary event? Careful scrutiny of ADPKD kidneys revealed that elevated levels of polycystin were only found in ~90% of all cysts. This observation suggests that polycystin overexpression is not the primary cause of cyst formation; rather, polycystin overexpression and cyst formation may both result from the same underlying failure to maintain appropriate epithelial differentiation. Indeed, several features of cystic epithelia have been linked to a de-differentiated state (22). In normal development, polycystin is most abundantly expressed in fetal kidneys; polycystin overexpression in ADPKD may simply reflect failure to maintain the mature state and a reversion, in cystic epithelia, to a state that is closer to the fetus.

ADPKD is a systemic disease involving cystic lesions in liver and pancreas as well the kidney. Northern analyses have shown that the *PKD1* transcript is found in many tissues (19). Here we show that the expression of polycystin is restricted to the epithelial cells in each of the tissues we studied. In fetal liver and pancreas, expression is confined to the biliary and pancreatic ducts. This pattern fits well with the origins of hepatic and pancreatic cysts in the small biliary and pancreatic ducts. Polycystin is not, however, confined to tissues which produce symptoms in ADPKD. It is abundant, for example, in basal keratinocytes and hair follicles of the skin, which are not reported to be abnormal in ADPKD. One of the established complications of ADPKD is intracranial aneurysm. Although we did not detect polycystin expression in blood vessels in the kidney, liver, pancreas or skin, it is possible that cerebral or larger arteries express polycystin.

A recent study of polycystin distribution using an antibody against a fusion protein showed a similar pattern to our findings in the kidney (23). However, the authors did not ascertain the subcellular location of polycystin, nor did they determine the size of the native molecule.

Localization of polycystin to plasma membrane focuses attention on the extracellular compartment as the site for interaction between polycystin and its ligand(s). Identification of the ligands will be a key step in our understanding of the function of polycystin and the pathogenesis of ADPKD.

Acknowledgments

We thank Dr. Harold Chapman for helpful discussion, Drs. Bjorn Olsen and Ramzi S. Cotran for support and encouragement, and the Coleman Family Fund for support.

This work was supported by National Institutes of Health grants DK-40703 to S.T. Reeders and DK-51050 to J. Zhou, and the PKR foundation. B. Peissel was supported, in part, by the Associazione Italiana per la Ricerca sul Cancro foundation.

References

1. Gabow, P.A., A.M. Johnson, W.D. Kaehny, W.J. Kimberling, D.C. Lezotte, I.T. Duley, and R.H. Jones. 1992. Factors affecting the progression of

- renal disease in autosomal-dominant polycystic kidney disease. *Kidney Int.* 41: 1311-1319.
2. Gabow, P.A. 1990. Autosomal dominant polycystic kidney disease — more than a renal disease. *Am. J. Kidney Dis.* 16:403-413.
3. Reeders, S.T., M.H. Breuning, K.E. Davies, R.D. Nicholls, A.P. Jarman, D.R. Higgs, P.L. Pearson, and D.J. Weatherall. 1985. A highly polymorphic DNA marker linked to adult polycystic kidney disease on chromosome 16. *Nature (Lond.)* 317:542-544.
4. Kimberling, W.J., S. Kumar, P.A. Gabow, J.B. Kenyon, C.J. Connolly, and S. Somlo. 1993. Autosomal dominant polycystic kidney disease: localization of the second gene to chromosome 4q13-q23. *Genomics.* 18:467-472.
5. Fosdall, R., M. Bothvarsson, P. Asmundsson, J. Ragnarsson, D. Peters, M.H. Breuning, and O. Jensson. 1993. Icelandic families with autosomal dominant polycystic kidney disease: families unlinked to chromosome 16p13.3 revealed by linkage analysis. *Hum. Genet.* 91:609-613.
6. Daoust, M.C., D.M. Reynolds, D.G. Bichet, and S. Somlo. 1995. Evidence for a third genetic locus for autosomal dominant polycystic kidney disease. *Genomics.* 25:733-736.
7. International PKD Consortium. 1995. Polycystic kidney disease: the complete structure of the *PKD1* gene and its protein. *Cell.* 81:289-298.
8. Hughes, J., C.J. Ward, B. Peral, R. Aspinwall, K. Clark, J. San Millan, V. Gamble, and P.C. Harris. 1995. The polycystic kidney disease 1 (*PKD1*) gene encodes a novel protein with multiple cell recognition domains. *Nat. Genet.* 10: 151-160.
9. Tokayasu, K.T. 1989. Use of poly(vinylpyrrolidone) and poly(vinyl alcohol) for cryoultramicrotomy. *Histochem. J.* 71:894-906.
10. Griffiths, G., A. McDowall, R. Back, and J. Dubochet. 1984. On the preparation of cyosections for immunocytochemistry. *J. Ultrastruct. Res.* 89:65-78.
11. Griffiths, G. 1993. Fine structure immunocytochemistry. Springer Verlag, Heidelberg. 417-436.
12. Carone, F.A., R. Bacallao, and Y.S. Kanwar. 1994. Biology of polycystic kidney disease. *Lab. Invest.* 70:437-448.
13. Wilson, P.D., A.C. Sherwood, K. Palla, J. Du, R. Watson, and J.T. Norman. 1991. Reversed polarity of Na⁺-K⁺-ATPase: mislocation to apical plasma membranes in polycystic kidney disease epithelia. *Am. J. Physiol.* F420-430.
14. Du, J., and P.D. Wilson. 1995. Abnormal polarization of EGF receptors and autocrine stimulation of cyst epithelial growth in human ADPKD. *Am. J. Physiol.* C487-495.
15. Wilson, P.D., and D. Falkenstein. 1995. The pathology of human renal cystic disease. *Curr. Top. Pathol.* 88:1-50.
16. Turco, A.E., S. Rossetti, E. Bresin, S. Corra, L. Gammara, G. Maschio, and P.F. Pignatti. 1995. A novel nonsense mutation in the *PKD1* gene (C3817T) is associated with autosomal dominant polycystic kidney disease (ADPKD) in a large three-generation Italian family. *Hum. Mol. Genet.* 4:1331-1335.
17. Peral, B., J. San Millan, A.C. Ong, V. Gamble, C.J. Ward, C. Strong, and P.C. Harris. 1996. Screening the 3' region of the polycystic kidney disease 1 (*PKD1*) gene reveals six novel mutations. *Am. J. Hum. Genet.* 58:86-96.
18. Peral, B., V. Gamble, J. San Millan, C. Strong, J. Sloane-Stanley, F. Moreno, and P.C. Harris. 1995. Splicing mutations of the polycystic kidney disease 1 (*PKD1*) gene induced by intronic deletion. *Hum. Mol. Genet.* 4:569-574.
19. European PKD Consortium. 1994. The polycystic kidney disease 1 gene encodes a 14 kb transcript and lies within a duplicated region on chromosome 16. The European Polycystic Kidney Disease Consortium. *Cell.* 77:881-894. (published erratum appears in *Cell* vol. 78 no. 4).
20. Reeders, S.T., K. Zerres, A. Gal, T. Hogenkamp, P. Propping, W. Schmidt, R. Waldherr, M.M. Dolata, K.E. Davies, and D.J. Weatherall. 1986. Prenatal diagnosis of autosomal dominant polycystic kidney disease with a DNA probe. *Lancet.* 2:6-8.
21. Baert, L. 1978. Hereditary polycystic kidney disease (adult form): a microdissection study of two cases at an early stage of the disease. *Kidney Int.* 13: 519-525.
22. Dvergsten, J., J.C. Manivel, R.R. Correa, and M.E. Rosenberg. 1994. Expression of clusterin in human renal diseases. *Kidney Int.* 45:828-835.
23. Ward, C.J., H. Turley, A.C.M. Ong, M. Comley, S. Biddolph, R. Chetty, P.R. Ratcliffe, K. Gatter, and P. C. Harris. 1996. Polycystin, the polycystin kidney disease 1 protein, is expressed by epithelial cells in fetal, adult, and polycystic kidney. *Proc. Natl. Acad. Sci. USA.* 93:1524-1528.